



City Research Online

City, University of London Institutional Repository

Citation: Sun, T., Fabian, M., Chen, Y., Vidakovic, M., Javdani, S., Grattan, K. T. V., Carlton, J., Gerada, C. & Brun, L. (2017). Optical fibre sensing: A solution for industry. Proceedings of SPIE, 10323, 103231H. doi: 10.1117/12.2272471

This is the accepted version of the paper.

This version of the publication may differ from the final published version.

Permanent repository link: <https://openaccess.city.ac.uk/id/eprint/18167/>

Link to published version: <https://doi.org/10.1117/12.2272471>

Copyright: City Research Online aims to make research outputs of City, University of London available to a wider audience. Copyright and Moral Rights remain with the author(s) and/or copyright holders. URLs from City Research Online may be freely distributed and linked to.

Reuse: Copies of full items can be used for personal research or study, educational, or not-for-profit purposes without prior permission or charge. Provided that the authors, title and full bibliographic details are credited, a hyperlink and/or URL is given for the original metadata page and the content is not changed in any way.

City Research Online:

<http://openaccess.city.ac.uk/>

publications@city.ac.uk

Optical fibre sensing: a solution for industry

T Sun^a, M Fabian^a, Y Chen^a, M Vidakovic^a, S Javdani^a, K T V Grattan^a, J Carlton^a, C Gerada^b and L Brun^c

^aCity University of London, Northampton Square, London EC1V 0HB, UK; ^bNottingham University, University Park, Nottingham NG7 2RD, UK; ^cFaiveley Brecknell Willis, Somerset TA20 2DE, UK

ABSTRACT

Optical fibres have been explored widely for their sensing capability to meet increasing industrial needs, building on their success in telecommunications. This paper provides a review of research activities at City University of London in response to industrial challenges through the development of a range of fibre Bragg grating (FBG)-based sensors for transportation structural monitoring. For marine propellers, arrays of FBGs mapped onto the surface of propeller blades allow for capturing vibrational modes, with reference to simulation data. The research funded by EU Cleansky programme enables the development of self-sensing electric motor drives to support 'More Electric Aircraft' concept. The partnership with Faiveley Brecknell Willis in the UK enables the integration of FBG sensors into the railway current-collecting pantographs for real-time condition monitoring when they are operating under 25kV conditions.

Keywords: FBG sensors; marine propeller; electric motor; pantograph

1. INTRODUCTION

An intensive review of the use of fibre optics for structural condition monitoring has been undertaken [1] showing a number of techniques, amongst which the most widely used are Fibre Bragg Grating (FBG)-based techniques [2]. FBGs produce wavelength encoded signals which are not susceptible to instrumental drift and environmental interference and have proven to be more robust and reliable, suitable for operation in harsh working conditions. The underpinning sensing mechanism of a FBG is that its Bragg wavelength (λ_B) shift is determined by the change in surrounding temperature and/or strain applied as described in equation (1) [3].

$$\frac{\Delta\lambda_B}{\lambda_B} = (1 - P_e)\epsilon + [(1 - P_e)\alpha + \zeta]\Delta T \quad (1)$$

where P_e is the photoelastic constant of the fibre, ϵ is the strain induced on the fibre, α is the fibre thermal expansion coefficient and ζ is the fibre thermal-optic coefficient. The first term of equation (1) represents the longitudinal strain effect on the FBG and the second term represents the thermal effect, which comprises a convolution of thermal expansion of the material and the thermal-optic effect. Equation (1) also indicates clearly the cross-sensitivity of a FBG to strain and to temperature, therefore when strain measurement is required using a FBG, its temperature effect is required to be compensated through optimizing the sensor design and sensor packaging.

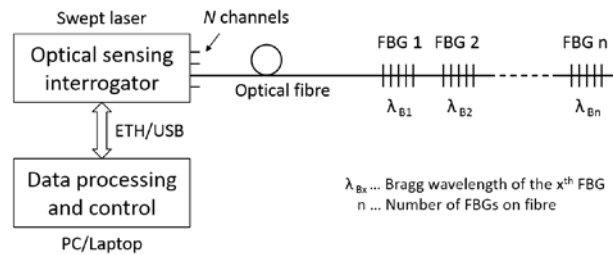


Figure 1. Quasi-distributed FBG sensor system using wavelength-division-multiplexing technique

One of the key features that FBGs offer is their multiplexing capability by using Wavelength Division Multiplexing (WDM) technique [4] to identify an array of FBGs written into a single length of fibre, each being encoded with a unique wavelength for ease of identification. The sensor interrogation can be achieved using a swept laser-based wavelength scanning technique as shown in Figure 1.

2. FIBRE OPTIC VIBRATION SENSORS

As indicated in equation (1), the Bragg wavelength shift is linearly proportional to the strain, the variation of which can be induced by the vibration of the object to which the FBG is attached. In this research, a full-scale marine propeller as shown in Figure 2 (a) is fully instrumented with 335 FBGs with each blade being mapped with 67 sensors using the layout shown in Figure 2 (b) in order to investigate their vibration behaviour both in air and underwater. The individual vibration frequencies at each measurement point is determined by the vibration signal captured by the FBG located at that specific position. Using this approach, a broader vibration pattern for each of the blades can thus be obtained.

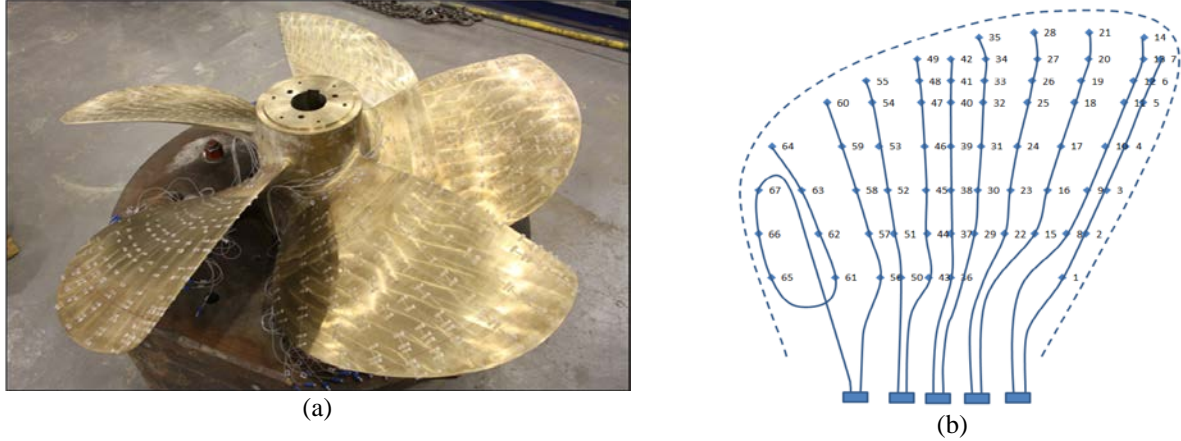


Figure 2. (a) a propeller with all the blades instrumented with a FBG-based sensor network; (b) layout of FBG sensors on each propeller blade

Table 1. Cross-comparison of the frequency elements derived from experimental data and from simulation of a propeller

| Left-Handed Propeller (K39047) Frequency Range (Hz); Experiment (air) | | | | | | | | | | | | |
|---|------|-------|-------|-------|-------|-------|-------|-------|-------|-------|-------|-------|
| Mode No. | 1 | 2 | 3 | 4 | 5 | 6 | 7 | 8 | 9 | 10 | 11 | 12 |
| Blade 1 | 93 | 214 | 222 | 374 | 403 | 501 | 568 | 585 | 632 | 757 | 831 | 862 |
| Blade 2 | 94 | 214 | 223 | 383 | 405 | 503 | 577 | 584 | 636 | 772 | 849 | 909 |
| Blade 3 | 94 | 213 | 231 | 378 | 403 | 501 | 576 | 587 | 637 | 768 | 830 | 897 |
| Blade 4 | 93 | 215 | 231 | 380 | 403 | 501 | 576 | 586 | 632 | 788 | 817 | 887 |
| Blade 5 | 93 | 214 | 222 | 375 | 399 | 501 | 568 | 585 | 632 | 757 | 807 | 867 |
| Left-Handed Propeller (K39047) Frequency Range (Hz); Simulation (air) | | | | | | | | | | | | |
| Mode No. | 1 | 2 | 3 | 4 | 5 | 6 | 7 | 8 | 9 | 10 | 11 | 12 |
| Blade 1 | 91.2 | 206.4 | 222.3 | 355.9 | 394.3 | 511.1 | 561.9 | 571.3 | 629.2 | 772.4 | 827.2 | 868.8 |
| Blade 2 | 90.7 | 208 | 220.4 | 370 | 388.8 | 513.9 | 566.6 | 569.4 | 639.1 | 778.7 | 830.3 | 890.2 |
| Blade 3 | 90.2 | 205.6 | 224.2 | 365.3 | 394 | 505.8 | 565 | 572.1 | 630.7 | 768.1 | 834.6 | 885.8 |
| Blade 4 | 88.5 | 209.2 | 225.4 | 367.4 | 402.2 | 508.2 | 573.4 | 585.1 | 629.6 | 771.5 | 842.7 | 887.2 |
| Blade 5 | 90 | 209.7 | 224.9 | 368.1 | 396.8 | 497.8 | 563.4 | 570.5 | 624.8 | 752.3 | 818.1 | 867.9 |

Table 1 shows a detailed cross-comparison of a series of vibrational modes of the propeller obtained from the experimental data using FFT analysis of the Bragg wavelength shifts of all the FBGs and from the finite element model created using the ANSYS software. A close agreement has been obtained and the small deviation that has been observed in the results is due to the fact that there is a small discrepancy between the geometric profile of the blades tested and those in the simulation model used. Subsequently the instrumented propeller was immersed in water and the vibration patterns obtained show that the same modes of vibration are present, although for some natural frequencies, the mode order is seen to be changed from one blade to another on the same propeller [5].

3. SELF-SENSING ELECTRIC MOTOR

A self-sensing PMAC electric motor, as shown in Figure 3, has been successfully developed under the EU Cleansky programme. This is achieved through integration of a novel all-in-one optical fibre sensor system, which comprises of 4 fibres carrying 48 FBGs, into a PMAC motor, provided by Nottingham University. In order to measure vibration, rotational speed and rotational position, one fibre carrying 12 FBGs is installed circumferentially around the stator core at the machine's non-drive end with FBGs being located in between 12 stator teeth. For stator thermal profiling, two fibres carrying 24 FBG sensors are installed with two sensors per stator slot. At the end of the stator core the fibres are looped around, skipping one slot at a time. The rotor information is captured by using one fibre carrying 12 FBGs installed onto the rotor, with 10 FBGs monitoring the magnet temperatures (one FBG per magnet) and other two being attached to the rotor shaft at an angle of $\pm 45^\circ$ to measure torque and the shaft temperature at that location [6]. A fibre-optic rotary joint shown in Figure 3 is used to couple the FBG signals from the rotor to the interrogator.

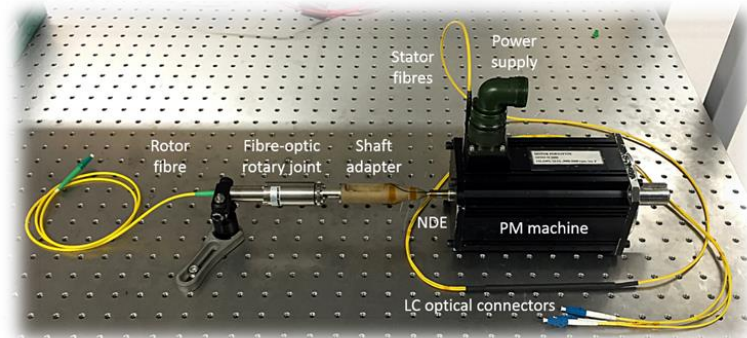


Figure 3. PM machine instrumented with 48 FBGs on 4 fibres measuring rotor speed, torque, vibration, the rotor magnet temperatures and stator end-winding temperatures.

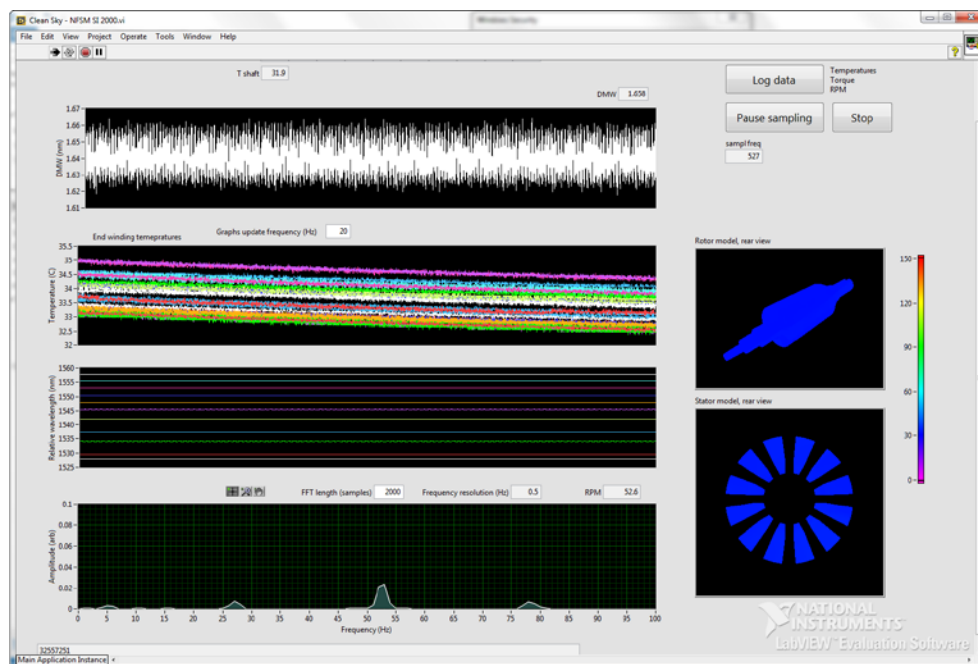


Figure 4. Interface of a temporary motor monitoring application at runtime showing key motor parameters.

Figure 4 shows a typical interface designed for end-users. The top left graph shows the differential mode wavelength of the torque sensor and this corresponds to the continuous torque values after calibration. The second left graph from the top shows the stator end-winding temperatures based on the wavelength shifts of the arrays of gratings mapped inside the stator as a result of temperature variation with time. The third left graph from the top shows the Bragg wavelength shifts

of the FBG mounted along the stator circumference needed to assess the dynamic response of those FBGs for precise rotor speed/position monitoring. The bottom left graph shows the stator vibration signature captured by the circumferentially mapped FBGs. The two graphs on the right visualise the rotor and stator temperatures in the form of colour coded 3D surface models, based on the sensor data obtained from the FBGs mounted on to the PMAC rotor/stator.

4. SMART PANTOGRAPH

The pantograph is a critical, roof-mounted part of a modern electric train, tram or electric bus to collect power through an overhead catenary wire and successful current collection requires a reliable pantograph-catenary contact with a *steady* force under *all conditions*, as the train travels along the line. The pantograph operates in a particularly harsh environment, being exposed to all weathers as its carbon strip rubs along the OLE at speeds up to 125 mph and at 25,000 volts conditions: monitoring its condition in real-time has posed a real technical challenge to the rail industry and optical fibre sensing provides an effective solution. Figure 5 shows a pantograph integrated with arrays of FBGs, which have been designed and configured to allow both real-time measurement of the contact force and contact location and facilitate a closed-loop control to avoid unexpected failure of pantograph during operation. This is a joint development between City University of London and Faiveley Brecknell Willis in the UK.



Figure 5. Calibration of a smart pantograph integrated with FBGs in industrial context

5. SUMMARY

A range of FBG-based optical fibre sensor systems have been developed and evaluated, showing promise for wide industrial applications. These sensors have been designed to provide real-time measurement of a suite of key parameters that would help engineers to diagnose structural conditions thus to improve structural integrity and reliability through improved maintenance.

ACKNOWLEDGEMENT

The authors would like to thank the financial support from RSSB in the UK and the EU Cleansky programme to enable the above research to be undertaken.

REFERENCES

- [1] Merzbacher, C. I., Kersey, A. D. and Friebele, E. J., "Fibre optic sensors in concrete structures: a review" in *Optical Fiber Sensor Technology* (Eds Grattan, K.T.V. and Meggitt, B.T.), 3, 1-24 (1999).
- [2] Kerrouche, A., Boyle, W.J.O., Sun, T., Grattan, K.T. and et al.. *Sensors and Actuators A - Physical*, 151(2), 107-112 (2009)
- [3] Pal, S., Shen, Y., Mandal, J., Sun, T. and Grattan, K.T.V. *IEEE Sensors Journal*, 5(6), 1462-1468 (2005).
- [4] Othonos, A. and Kalli, K., "Fiber Bragg gratings: fundamentals and applications in telecommunications and sensing". *Artech House Boston* (1999).
- [5] Javdani, S., Fabian, M., Carlton, J. S., Sun, T. and Grattan, K. T. V. *IEEE Sensors Journal*, 16 (4), 946-953 (2016).
- [6] Swart, P. L., Chtcherbakov, A. A. and Van Wyk, A. J., *Meas. Sci. Technol.* 17(5), 1057-1064 (2006)